Two-Dimensional Diffusion of Prodan on Self-Assembled Monolayers Studied by Fluorescence Recovery after Photobleaching

Carla E. Heitzman, Huilin Tu, and Paul V. Braun*

Department of Materials Science and Engineering, Beckman Institute for Advanced Science and Technology, and Frederick Seitz Materials Research Laboratory, University of Illinois at Urbana−Champaign, 1304 West Green Street, Urbana, Illinois 61801

Received: April 24, 2004; In Final Form: June 20, 2004

Fluorescence recovery after photobleaching (FRAP) is used to determine diffusion constants for the dye molecule 6-propionyl-2-dimethylaminonaphthalene (prodan) on silica and on a variety of organic monolayers grafted onto silica. Similar diffusion constants of $\sim 2 \times 10^{-7}$ cm^2/s are found for prodan on chlorotrimethylsilane (CTS) based self-assembled monolayers and on silanated poly(ethylene glycol) based monolayers. The similar diffusion constants are intriguing given the different surface free energies of these surfaces. No dye recovery is observed on octadecyltrichlorosilane (OTS) based monolayers or on clean silica surfaces. No significant change in the diffusion constant is observed with varying relative humidity on any of the surfaces. A mechanism for the diffusion of dye on these four surfaces is discussed. A simple surface energy argument may explain why diffusion is extremely limited on both very hydrophobic and very hydrophilic surfaces, but is allowed on surfaces with intermediate polarities. Additionally, we suggest, in the case of CTS vs OTS based monolayers, that the presence of disorder in the CTS based monolayer is important for rapid diffusion. Similar concepts are presented for the other systems examined.

Introduction

Two-dimensional (2D) diffusion is a relevant and interesting topic of study in many scientific fields. In the surface science community, examples of diffusion studies abound centered on topics such as the "Brownian motion of 2D vacancy islands by adatom terrace diffusion,"[1] and "non-nearest-neighbor jumps in 2D diffusion."[2] In biology, the diffusion of lipid molecules *in* supported membranes[3] and the conformation and diffusion of DNA molecules *on* lipid bilayers[4] are of current interest. Other soft-matter systems include diffusion in dense two-dimensional liquids,[5] diffusion in two-dimensional glasses,[6] and two-dimensional diffusion of point defects in colloidal crystals.[7] The specific studies we undertake in this paper are of two-dimensional diffusion of small fluorescent molecules on and in self-assembled monolayers (SAMs)[8,9] and on bare glass. Because the grafted molecules comprising the SAM are covalently attached to the substrate, they are immobile, and thus the local environment is fundamentally different than that in lipid diffusion studies. This paper presents the first results on the solid state (solvent-free) translational diffusion of small, unattached molecules in a layer of grafted molecules or oligomers.

For inorganic studies, scanning tunneling microscopy and other high vacuum surface science techniques have proved to be very powerful tools. In biological and polymeric systems, entirely different classes of tools, primarily centered around fluorescence imaging, have been developed.[10,11] In some cases, characterization of diffusion in organic systems can also be accomplished using traditional solid state techniques,[12,13] however, fluorescence-based approaches are more popular.[3,14,15] For instance, in polymer systems, motion of individual polymer molecules can be monitored by tagging with a fluorescent probe.[16−18] Alternatively, polymer segmental motion and side chain dynamics can be inferred by measuring the diffusion of appropriately sized fluorescent probes dissolved in a polymer melt. Torkelson's group has used fluorescence nonradiative energy transfer to perform such studies.[19,20] Two layers of the same polymer, one containing a dye molecule and the other containing an acceptor molecule, are formed one on top of the other; diffusion of the probe molecule results in decreased fluorescence due to quenching of the dye by the acceptor, and thus diffusion rates can be calculated from fluorescence intensity measurements. Fluorescence correlation spectroscopy can be used to measure diffusion of very small concentrations of a bright, stable (hard to bleach) probe molecule.[16,21,22] The diffusion of individual probe molecules into and out of the illuminated volume results in fluctuations in fluorescence intensity. From the correlation of this signal over time, along with the known concentration, the diffusion rate of the probe molecule can be calculated.

Fluorescence recovery after photobleaching (FRAP) is a straightforward way to measure diffusion of dye molecules that are easily bleached and not sufficiently bright for single molecule detection.[14,15] It is the primary characterization technique used in this paper and is often used to measure diffusion in membranes and other biological systems.[3,15] For our system, FRAP studies are performed by first depositing dye uniformly over the sample. A defined area of the sample is illuminated with photons of an appropriate energy to excite the dye and at a sufficient power to bleach a measurable fraction of the dye molecules. After bleaching, images are collected as a function of time (Figure 1). Fluorescence recovery in the bleached region is due to diffusion of "live" dye molecules into the bleached area, and thus a diffusion rate can be calculated from the recovery rate.

Transport *through* the interior of a polymer brush requires sufficient segmental mobility to enable rapid diffusion of dissolved molecules or ions.[23] Thus, a low glass transition

* Corresponding author. Telephone: (217) 244-7293. Fax: (217) 333-2736. E-mail: pbraun@uiuc.edu.

10.1021/jp048202v CCC: $27.50
Published on Web 08/17/2004

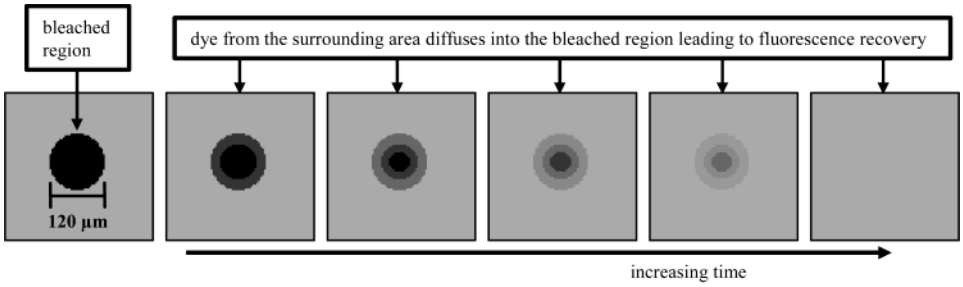

Figure 1. Schematic images of fluorescence recovery as a function of time.

temperature and high side chain mobility are desired qualities. If the transport kinetics are not adequately fast, it may be possible to plasticize the polymer brush or monolayer,[24] for example by swelling the layer with water or other molecules,[25,26] to enable transport. For successful transport *on* a polymer surface, the dynamics of the polymer may not be as important. Rather, the interaction potential of the molecule and the layer must be sufficiently strong to prevent aggregation of the molecule, yet weak enough to allow the molecule to diffuse. Similar interaction potentials are necessary for transport on SAMs as well. Other relevant parameters may include the packing density, regularity, and surface coverage of the SAM. These factors, along with the size and chemistry of the diffusing species,[20] may have a great impact on the rate of diffusion.

This paper reports and discusses diffusion results of a dye molecule, 6-propionyl-2-dimethylaminonaphthalene (prodan, **1**), on or in three organic surfaces and a bare surface: silanated poly(ethylene glycol) (PEG), chlorotrimethylsilane (CTS), and octadecatrichlorosilane (OTS) grafted to silica, and clean (piranha-treated) silica. The silica surface is hydrophilic, even relative to the PEG layer, due to a high concentration of silanol groups;[27] the CTS and OTS based surfaces are both hydrophobic but differ from each other in the shape, thickness, and density of the monolayer, the water contact angle, and the number of possible bonds per molecule to the surface. Prodan was selected because it is small, and thus probably will diffuse more rapidly than large dyes; it is polar, and thus may dissolve or disperse on polar surfaces; and, importantly, it can be excited and bleached though a multiphoton process using infrared radiation. The effects of relative humidity and dye concentration have also been studied. The relative humidity in nitrogen was varied from 0% to 90% to determine what, if any, effect this has on diffusion; dye concentration was varied to identify the range of concentrations large enough to provide sufficient fluorescence for detection without resulting in unrecoverable fluorescence after photobleaching, presumably from immobile dye.

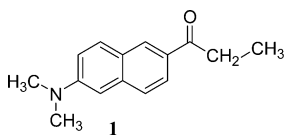

1

In addition to fundamental studies, this work may serve as the first step toward the transport of molecular species through patterned structures, which may be quite interesting as a new paradigm for defined molecular transport. This concept could be of use for example for the interfacing of traditional microelectronic devices with chemical and biological structures. Successful design of two-dimensional chemical pathways or "molecular conduits" on a surface will require a thorough understanding of the dynamics of diffusion of small molecules on surfaces and the development of surfaces on which rapid diffusion exists and surfaces on which slow, near-zero diffusion exists. Self-assembled monolayers and other thin films of functionalized (small or polymer) molecules chemically attached to the substrate may be ideal structures for both the molecular conduits and the insulating layers. A variety of techniques are available for creating and defining covalently grafted structures on surfaces including microcontact printing,[28,29] photolithography,[30] embossing,[31] and ink-jet printing.[32] With these methods, features such as lines and dots ranging from 1 nm to 100 nm thick and 10 nm to microns wide can be created over large areas.

Experimental Section

The surfaces examined were the following: glass reacted with CTS, OTS, or end-functionalized PEG and piranha-treated glass. All chemicals were used as received from Acros unless otherwise indicated.

Synthesis of Silane-Functionalized PEG. The synthesis was adapted from published procedures.[33,34] Poly(ethylene glycol) methyl ether (m-PEG, average M_n ca. 2000) and dibutyltin dilaurate were purchased from Aldrich. 3-Isocyanatopropyltriethoxysilane (IPTS) was purchased from Gelest. Briefly, m-PEG (20 g, 0.01 mol) was dissolved in 150 mL of toluene in a 250 mL round-bottomed flask. Through azeotropic distillation 120 mL of toluene and as much water as possible were distilled out of the mixture. Then 100 mL of dry THF (distilled over CaH_2) was added to the mixture. IPTS (2.5 mL, 0.01 mol) and dibutyltin dilaurate (0.23 mL, 0.4 mmol), dissolved in 20 mL of dry THF, were added dropwise to the m-PEG solution while stirring with a magnetic stirrer. The reaction mixture was stirred continuously for 48 h at room temperature under dry nitrogen. After the reaction, the silanated PEG 2000 (**2**) was precipitated twice with petroleum ether, and then dried in vacuo. A white powder was obtained after drying. NMR, IR, and GPC confirmed the chemical structure of **2** ($n \sim 45$).

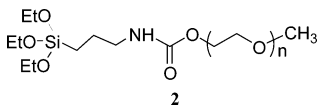

2

Sample Preparation. Samples were made on Fisherbrand microscope cover glasses (22 mm × 22 mm × 0.17 mm). These were cleaned by submersion in boiling piranha solution (3:1 v/v H_2SO_4 and H_2O_2; 30% aqueous solution) for 18 h. They were subsequently rinsed five times in Millipore deionized water (18.2 MΩ·cm) and dried with nitrogen. Monolayers were formed from CTS and OTS (Aldrich) by submerging cleaned coverslips in solutions of 20 mL of hexane and 40 μL of OTS or CTS for 1 h. Samples were then sonicated in hexane for 1 h to remove excess material from the surface and subsequently rinsed in hexane, ethanol, and finally deionized water before being dried with nitrogen.

PEG layers were formed using the functionalized PEG **2**. A 100 mg sample of **2** was dissolved in 20 mL of ethanol and 1 mL of water; hydrochloric acid was added until a drop of the solution turned pH paper a color corresponding to pH 2. The substrates remained in solution for 2 days at room temperature and were subsequently rinsed with ethanol and deionized water and blown dry with nitrogen.

Layer Characterization. Monolayers of all the above molecules were also formed on silicon wafers covered with their native oxide, following an identical procedure, for ellipsometric thickness measurements (Gaertner Scientific Corporation, Model L116c). The thickness of the native oxide was subtracted from the measured thickness of the deposited layer. In calculating the layer thickness, a substrate index of refraction of 3.85, a layer index of 1.46, a substrate extinction coefficient of −0.02, and a layer extinction coefficient of 0 were assumed. Contact angle measurements of water on the surfaces studied were taken of samples made on both the wafers and the coverslips using a Rame-Hart goniometer (Model 100-00).

Dye Deposition. Organic layers made on coverslips were used for all diffusion studies. Solutions of prodan in ethanol were spin-coated (Speedline Technologies, Specialty Coating Systems, Inc., Model P6204) onto the layers at 2000 rpm. The concentration of prodan in solution was measured with a spectrometer (Shimadzu UV-1601PC). An absorption spectrum was taken from 250 to 500 nm; the peak absorption of prodan is at 360 nm with an extinction coefficient of 18 400 cm^{-1} M^{-1}. Solution concentration was calculated with the Beer−Lambert equation:[35]

$$A = \log\left(\frac{I_0}{I}\right) = \epsilon c d \tag{1}$$

The absorbance, A, is equal to the logarithm of the ratio of the intensity of impingent light, I_0, divided by the intensity of transmitted (not absorbed) light, I. From absorbance, the dye's extinction coefficient, ϵ,[36] and the sample path length, d (1 cm), the solution concentration, c, can be calculated. The thickness of the spin-coated layer, h, can be estimated from the solvent used and the spin speed using the following equation:[37]

$$h = \left(\frac{3\eta m}{2\rho\omega^2}\right)^{1/3} \tag{2}$$

The viscosity, η, and density, ρ, of ethanol, the solvent used, are known.[38] The evaporation rate, m, of ethanol was taken from the literature.[39] The rotational rate, ω (radians per second), was calculated from the revolutions per minute (rpm) spin speed as follows:

$$\omega = \text{rpm}\,\frac{2\pi}{60} \tag{3}$$

From the thickness of the ethanol layer and the dye concentration, the amount of dye deposited on the surface can be calculated as follows:

$$C_S = hcN_A \tag{4}$$

C_S is the surface concentration (molecules per area), h is the layer thickness, c is the solution concentration (moles per volume), and N_A is Avogadro's number. This route to estimate prodan concentration was used because the amount of dye deposited is too small to detect with UV−vis absorption measurements and prodan's emission yield is dependent on the environment.[40] Therefore, fluorescence is not an appropriate method to measure dye concentration.

For the samples in this study, the solvent was ethanol and the spin speed was 2000 rpm. The dye solution concentration ranged from 10 to 35 μM. These concentrations are sufficiently low such that the viscosity, density, and evaporation rate of pure ethanol can be used to calculate the dye solution thickness. Complete surface coverage of a dye layer one molecule thick corresponds to ∼0.84 prodan molecule/nm^2. The 10 and 35 μM prodan solutions in ethanol, spin-coated at 2000 rpm, correspond to 0.02 and 0.07 prodan molecule/nm^2, surface coverages of 2.4% and 8.3%, respectively.

Sample Cell. Diffusion was measured in a cell designed to fit on the confocal microscope and maintain an oxygen-free nitrogen atmosphere with a variable relative humidity. An O-ring was placed over the relevant sample surface and a Plexiglas cover was screwed down on top. The Plexiglas had an inlet and outlet that allowed for a gas flow during the course of the experiment. An Omega flowmeter (Model FL-3AB45G61-G61GHRV) was used to combine dry nitrogen and nitrogen with 90% relative humidity. The latter was flowed through a bubbler; the resulting relative humidity was measured with a Fisherbrand traceable humidity meter (Model 92-4185-00). The combined flow rate through the sample holder, which had a volume of about 1 cm^3, is about 1 cm^3/s.

Fluorescence Recovery after Photobleaching. Diffusion coefficients were quantified by measuring the fluorescence recovery after photobleaching (FRAP). Images were acquired with a Leica confocal microscope (Model TCS SP2). A 63× oil immersion objective was used. The field of view is 238 μm × 238 μm, and the circular bleached area has a diameter of 119 μm and was located in the center of this viewing region. The dye was excited (for both bleaching and imaging) with a mode locked Ti:sapphire laser tuned to 780 nm, with a pulse width of ∼57 fs. The beam was modulated with an electrooptical modulator (EOM). The laser power was ∼400−500 mW before it entered the microscope and ∼100 mW at the focal point. A circular area was bleached by rastering the beam and selectively blocking it with the EOM. Bleaching was performed until the observed fluorescence did not change. This took ∼10 s (∼6 scans) for the lower dye concentrations and up to 30 s at the highest dye concentration. Because of the dark noise in the PMT, the signal intensity did not go to zero. The effect of the finite bleaching time on the diffusion measurements will be discussed. Subsequent images were taken at time intervals relevant to the specific system: shorter time intervals were used for systems with faster diffusion. Bleaching was done with a field of view of 119 μm × 119 μm, while imaging was done using a field of view of 238 μm × 238 μm; thus the power density is decreased by a factor of 4, minimizing bleaching during data acquisition. The background intensity did not decrease significantly during imaging, leading to the conclusion that bleaching during imaging is not a significant problem.

Image Analysis. Images of the fluorescence recovery for each system were analyzed with a program written in C (see Supporting Information) to yield distance (from the center of the image) versus intensity curves for each time imaged. The curves for a specific system were all plotted on the same graph (see Figure 3b). The intensity value for a given radius is defined as an average of the intensities of all of the pixels located in the ring determined by the radius ± 2.32 μm (5 pixels). Pixel intensities ranged from 0 (black) to 255 (white). Each pixel was counted only once. The experimental series of curves was compared to a series of curves generated on

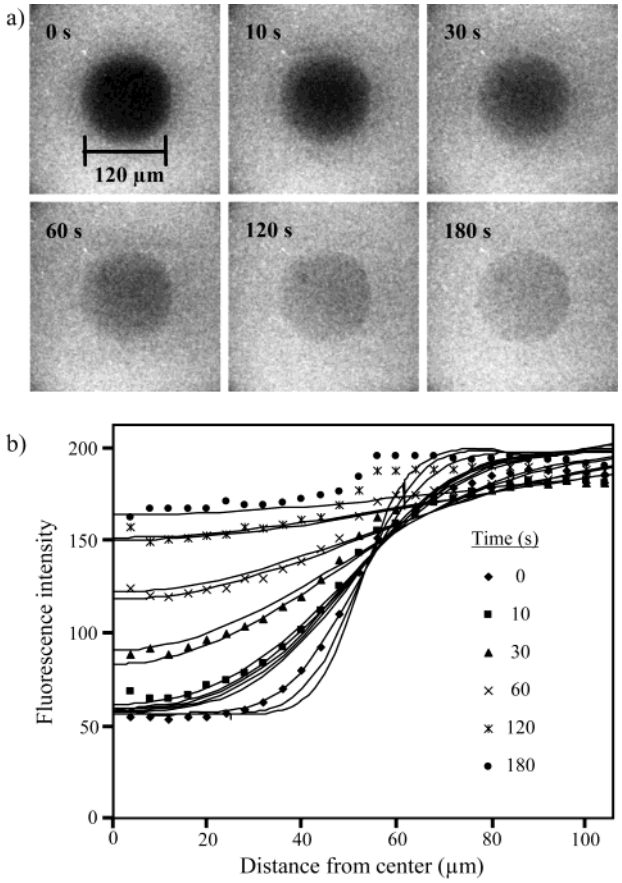

Figure 2. FRAP on PEG surfaces at a prodan concentration of 0.07 prodan molecules/nm^2. (a) Two-photon imaging of fluorescence recovery. (b) Experimental (symbols) and simulated (lines) intensity vs radial position as a function of time. Simulated data are for $D = 1.8 \times 10^{-7}$ cm^2/s at varying time offsets ranging from 1 to 5 s. The offsets for the $t = 0$ data are 2, 3, and 5 s; the offsets for the $t = 10$ s data are 0, 1, 2, 3, and 5 s. The next three pairs of simulated curves include only the 0 and 5 s offset; the topmost curve is for 180 s with no offset.

Mathematica (Wolfram Research Inc.) from eq 5, derived from Fick's second law of diffusion,[41] to determine the diffusion constant.

$$C(r,t) = C_0 - C_0 r_0 \int_0^\infty \mathrm{d}\alpha\, J_0(\alpha r)\, J_1(\alpha r_0) \mathrm{e}^{-\alpha^2 D t} \qquad (5)$$

Equation 5 is specifically for diffusion in an infinite cylinder and was used to create curves for our system which we modeled as diffusion into a two-dimensional circular area from an infinite plane. C_0 is the initial dye concentration on the sample, r_0 is the radius of the bleached region, D is the diffusion constant, and t is time. Curves of concentration, C, versus radius, r, were generated for the relevant times. J_0 and J_1 are Bessel functions. A more complete derivation of this equation can be found in the Supporting Information.

Results

Figure 1 is a schematic of a series of FRAP images as a function of time; actual FRAP images of PEG surfaces and an OTS surface are presented as Figures 2a, 3a, and 4a. Graphs of the radial fluorescence intensity as a function of time from these images are plotted in Figures 2b, 3b,c, and 4b. The radial fluorescence intensity as a function of time on a clean glass surface is presented as Figure 5. The diffusion constant of the dye on each surface is found by plotting a family of curves for a given value for D using eq 5 plus an offset time, selected as shown in Figure 2b. The quality of the fit is judged by eye, and subsequent (higher or lower) guesses for the diffusion constant and offset time are tested in a similar manner until a good fit is found. The maximum error in D we expect through this approach is $\pm 1 \times 10^{-7}$ cm^2/s (Figure 3c).

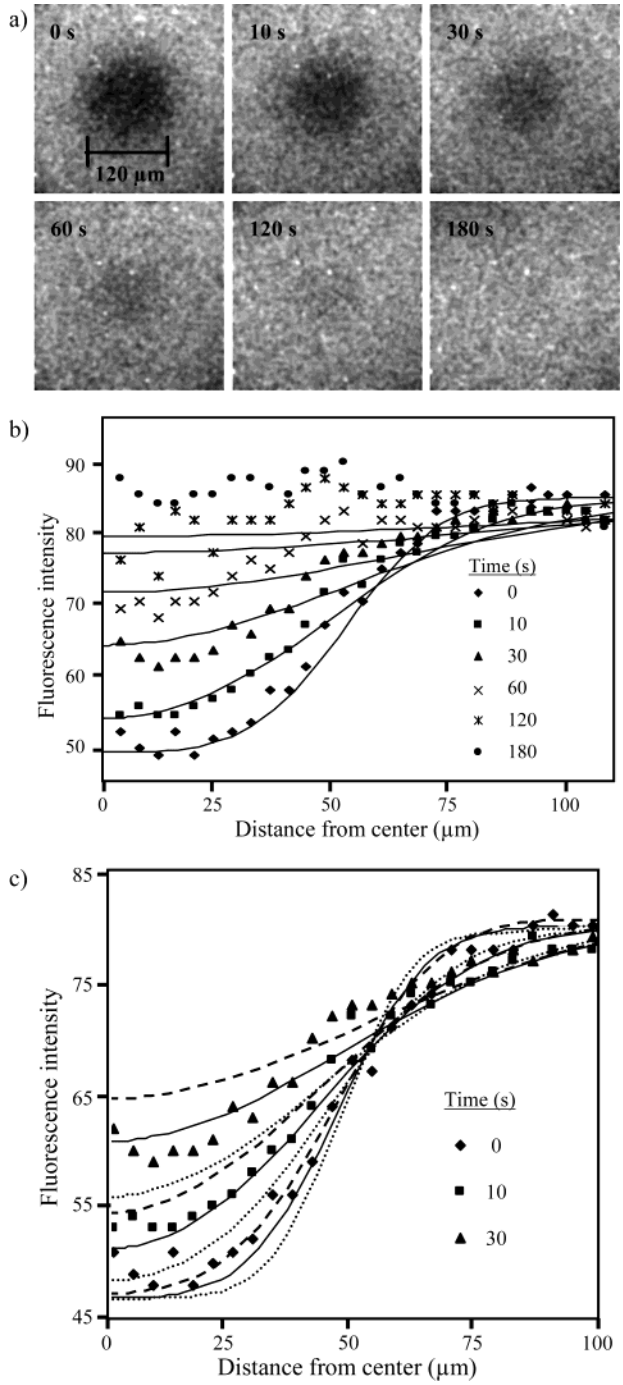

Figure 3. FRAP on PEG at a prodan concentration of 0.02 prodan molecules/nm^2. (a) Two-photon imaging of fluorescence recovery. (b) Experimental (symbols) and simulated (lines) intensity vs radial position as a function of time. Simulated data are for $D = 3 \times 10^{-7}$ cm^2/s with a time offset of 5 s. (c) Intensity vs position as a function of time with a time offset of 5 s, for varying values of D. The solid lines are for $D = 3 \times 10^{-7}$ cm^2/s; the dotted and dashed lines which lie below and above each solid line are for 2×10^{-7} and 4×10^{-7} cm^2/s, respectively.

Figure 2b illustrates the method for fitting a time offset for the curves: curves for offset times of 0, 1, 2, 3, and 5 s are all plotted. A time offset is necessary because the bleaching is not instantaneous. Instead, bleaching takes 10−30 s and so diffusion into the bleached area is occurring concurrent with bleaching.

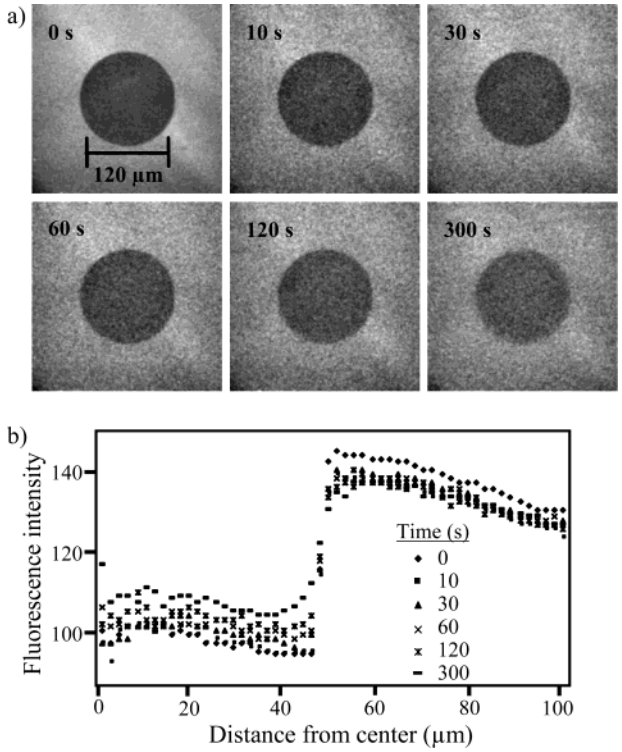

Figure 4. FRAP on OTS at a prodan concentration of 0.07 prodan molecules/nm^2. (a) Two-photon imaging of fluorescence recovery. (b) Intensity vs radial position as a function of time.

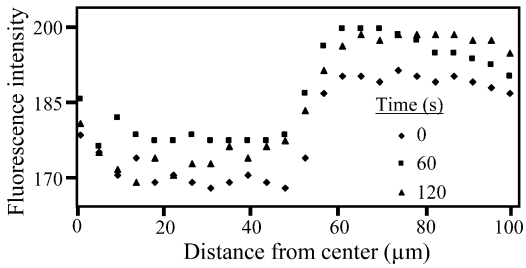

Figure 5. FRAP intensity vs position as a function of time for prodan, at a concentration of 0.07 prodan molecules/nm^2, on a clean cover glass.

This effect is compensated for by fitting the data from the "time = 0" image with a curve generated by setting the time equal to some time greater than 0, usually 5 s. The data from images taken at times greater than "time = 0" are likewise fit with curves that are offset by the same amount. As would be expected, this time offset has a diminished effect on the resulting curve at longer times, and by 120 s, the curves for 120 s and 120 + 5 s are almost indistinguishable.

Images and graphs for Figures 2 and 3 are both from prodan on PEG surfaces. The dye concentration in Figure 3 is lower than that in Figure 2 (spin-coated from 10 vs 35 μM prodan solutions in ethanol). The calculated diffusion constant is 3×10^{-7} cm^2/s for the lower dye concentration and 1.8×10^{-7} cm^2/s for the higher concentration. Figure 3c presents the calculated curves for three different D values, 2×10^{-7}, 3×10^{-7}, and 4×10^{-7} cm^2/s, along with the experimental data. It can be seen that 3×10^{-7} cm^2/s is the closest fit to the experimental data. Figure 4 shows the lack of measurable diffusion on OTS. A small amount of fluorescence recovery may be taking place; however, this cannot be fit with a diffusion equation and thus may be due to sublimation or more likely rotational diffusion of dye molecules, both of which would tend to increase the fluorescence in the bleached area uniformly. Figure 5 shows a graph of the radial fluorescence intensity taken from images of a clean surface. There appears to be little or no recovery on OTS or on clean glass. A minimum measurable value for D we could expect to measure is 5×10^{-10} cm^2/s.

TABLE 1: Prodan Diffusion Constants on Surfaces with Varying Relative Humidity

surface	relative humidity (%)	diffusion constant ($\times 10^{-7}$ cm^2/s)	no. of samples
PEG	0	1.8−3	4
PEG	45	2.5−3	2
PEG	90	2.5	1
CTS	0	1	3
CTS	22	1.8−2.5	2
CTS	30	1.8	2
CTS	45	1.8	2
OTS	0	<0.005	3
clean glass	0	<0.005	4

TABLE 2: Advancing and Receding Water Contact Angles and Thickness of the Surfaces

surface	contact angle (deg) advancing	contact angle (deg) receding	thickness (Å)
PEG	33 ± 0.5	14 ± 1.5	14 ± 2
CTS	70.5 ± 0.5	60.5 ± 0.5	3 ± 1
OTS	109 ± 1	93 ± 4	28 ± 2
clean glass	14 ± 1.5	0	NA

Table 1 lists the diffusion constants found for prodan on various surfaces under dry nitrogen as well as under nitrogen with varying levels of relative humidity. The number of independent experiments that were performed for each condition to determine the diffusion constant value or range of values is also included. The thickness, as measured with ellipsometry, and water contact angle for each surface are listed in Table 2.

Prodan diffusion on PEG in dry nitrogen is slightly faster than on trimethylsilane in dry nitrogen. Varying the level of relative humidity does not result in a significant difference in the measured diffusion on PEG. A slight increase, from 1×10^{-7} to 1.8×10^{-7} cm^2/s, in the diffusion rate is observed on the CTS surface at relative humidity levels greater than zero. Although the difference is within the error of one experiment, the measured diffusion constant on the CTS surface was highly reproducible, and thus we believe the difference is real. At higher dye concentrations, increased relative humidity also results in increased fluorescence for some of the surfaces, most noticeably the PEG. As dye concentration is lowered, the jump in fluorescence intensity with relative humidity decreases and ultimately disappears. At higher dye concentrations, the unrecoverable fluorescence after photobleaching is also greater for higher relative humidity on PEG.

Discussion

Most simply, our surfaces can be divided into two categories: surfaces on which prodan diffuses noticeably during the time scale of the experiment and surfaces on which it does not. The PEG and trimethylsilane surfaces fall under the first category, and the clean and OTS surfaces fall under the latter. In terms of thickness and contact angle, the two surfaces on which prodan does not diffuse represent both the thickest and most hydrophobic layer (OTS) as well as the thinnest and most hydrophilic layer (clean surface). If one assumes that diffusion takes place *on*, and not *in* and *through*, the layer, which may not be entirely true on the PEG surface, the surface free energy is a more important consideration than the thickness of the layer. It appears that the intermediate surface free energies of the PEG and the trimethylsilane surfaces, with water contact angles of 33° and 68°, respectively, are more conducive to prodan diffusion than the very low surface free energy of OTS, as

shown by its water contact angle of 109°, or the high surface free energy of clean glass, which has a water contact angle of 14°.

Prodan **1** is a relatively polar dye, containing both carbonyl and amine groups. It is about 5 times more soluble in methanol ($\sim 2.0 \times 10^{-2}$ M) than in the less polar solvent hexane ($\sim 4.4 \times 10^{-3}$ M). Thus, it is likely to aggregate on the hydrophobic OTS derived surface. The fluorescence intensity from the same concentration of **1** on the OTS derived surface is significantly lower than on the PEG or trimethylsilane surface, which is a strong indication of aggregation as dye aggregates are commonly known to self-quench.[42,43] We also sometimes observe bright dots on the OTS surface at higher dye concentrations. These "aggregates" are not observed on the PEG surfaces. It seems likely that diffusion of dye aggregates would be slower than that of well-dispersed small molecules; thus aggregation may be the reason no diffusion is observed on OTS during the time scale of the experiment. The reason, however, that diffusion is not observed on the clean hydrophilic silica surface is less clear; possibilities include aggregation and hydrogen bonding. The solubility limit of **1** in water is quite low (3.5×10^{-6} M), indicating that aggregation on a polar surface is possible. However, diffusion may be limited even if prodan molecules are well-dispersed because the piranha-treated glass surface contains a high concentration of silanol groups with which **1** can form hydrogen bonds, making the energy barrier for diffusion considerably higher than it is for the other surfaces. The low fluorescence intensity from the same concentration of **1** on a glass surface, compared to a PEG or CTS surface, may be due to either aggregation or hydrogen bond related quenching (as is thought to occur for the fluorescent amino acid tyrosine).[35]

The contact angles for water on the CTS derived surface ($\sim 70°$) and on the OTS surface (109°) give a strong hint as to why the diffusion rates for **1** are so different on the two surfaces. The difference in the contact angle is primarily due to the size and shape of the OTS and CTS molecules. Relative to OTS, CTS is a small, branched molecule and, unlike OTS, which can form three bonds with the substrate, CTS forms only one bond with the substrate. The three methyl units of an attached trimethylsilane molecule sterically inhibit attachment of additional CTS molecules, resulting in unreacted silanol groups on the substrate as well as inefficient and irregular packing of the molecules.[44] As a result, the 3 Å thick CTS derived layer may have pockets of partially exposed hydrophilic surface with which the prodan molecules can interact, thus improving their dispersion. However, because the majority of the surface is still coated with trimethylsilane, the prodan molecules are not as strongly bound as they are to the clean silica surface, and diffusion is possible. Unlike CTS, OTS efficiently packs on a surface, forming a layer that is measured to be ~ 28 Å thick which corresponds closely to the extended chain length of the molecule.[45] Because the resulting layer is both thicker and, presumably, better packed than the CTS derived surface, unreacted and exposed silanol groups and pockets are much less likely.

Our FRAP results on various surfaces lend some insight into the nature of the diffusion observed. The fact that there are surfaces on which there is no fluorescence recovery, specifically OTS and the clean glass, indicates that the observed recovery on other surfaces is due to diffusion and that the diffusion is indeed 2D in nature, and not through the overlying gas phase. If the fluorescence recovery was primarily due to dye molecules subliming and recondensing on the bleached region of the substrate, fluorescence recovery would be observed on at least the OTS surface, and probably on the clean glass surface as well. Although hydrogen bonding between prodan and the clean glass may be a barrier for sublimation as well as diffusion, hydrogen bonding cannot be present between the OTS surface and the dye, and thus recovery due to sublimation and recondensation would be expected to take place on that surface, if possible on any of the surfaces studied. The fact that the fluorescence recovery on the OTS surface is insignificant compared to that on the CTS or PEG functionalized surfaces rules out sublimation as a major contributor to the fluorescence recovery.

Our hypothesis for diffusion on the CTS surface suggests that the prodan molecules may be interacting with the surface, and thus are partially "in" the layer rather than strictly "on" it. Prodan molecules are roughly 17 Å long and 7 Å wide and the CTS SAM is about 3 Å thick, so the diffusing species must still exist mainly above the layer; however, the ability of prodan to partially interact with the underlying substrate may lead to a better dispersion of dye molecules on this surface than on OTS, which may lead to the greatly increased observed diffusion. On the PEG layer, which is 14 Å thick and probably amorphous, the possibility for partial insertion of the diffusing species is greater. As one extends to thicker and thicker layers, of PEG or other polymers, this question of "in" or "on" becomes increasing relevant and interesting to study.

The effect of relative humidity on the rate of diffusion was not substantial. On the PEG surface, the value of D determined from FRAP images taken from different spots on the same sample at the same relative humidity had as much variation (1.8×10^{-7} to 3×10^{-7} cm^2/s) as the value of D determined for different relative humidities, so it is impossible to determine a trend from these data. On the CTS surface, the difference in D between 0% and 25% relative humidity (and above) is small (1×10^{-7} vs 1.8×10^{-7} cm^2/s), but D at elevated relative humidity is consistently greater than D under completely dry nitrogen. Possibly, water molecules are interacting with exposed silanol groups which may block the prodan from hydrogen bonding with the substrate. Water could also decrease other barriers to prodan diffusion of which we are not yet aware.

The solubility of prodan in tetraglime, a molecule similar in chemistry to the PEG layers, is as high or higher than the solubility in methanol ($\sim 2.0 \times 10^{-2}$ M). We suspect that prodan solubility is high on and in the PEG layer as well, but at very high dye concentrations it may still be possible that aggregates are formed on PEG functionalized surfaces. This is supported by the experimental results of very high dye concentration on PEG: fluorescence intensity initially increases when the (bleaching) laser is shone upon it, and then decreases. In addition, full fluorescence recovery in the bleached area does not occur at high dye concentration. These effects are not observed at low dye concentrations (compare Figures 2a and 3a). The effect of humidity on PEG samples with high (>0.04 prodan molecule/nm^2) dye concentrations indicates aggregation as well: the fluorescence intensity, as well as the amount of unrecoverable fluorescence after photobleaching, increases with relative humidity. We think this is due to an incorporation of water in the PEG layer resulting in a greater dissolution of the prodan dye molecules (which are negligibly fluorescent when aggregated as a bulk solid in the dry state). At low enough dye concentrations, there is no increase in fluorescence intensity with relative humidity, and so we assume that the dye molecules are fully dispersed on/in the sample under dry nitrogen.

Finally, we compare the diffusion rates we observe in our system(s) with diffusion rates reported in the literature for similar

systems. Poly(ethylene glycol) was found to diffuse on the surface of an OTS monolayer with D decreasing from $\sim 10^{-8}$ to 10^{-10} cm^2/s, as the molecular weight increased from 2200 to 30 500 g/mol.[16,17] This is at least an order of magnitude lower than the D values we calculated for diffusion of **1** on CTS and PEG surfaces, but this is for diffusion of a polymer molecule that is at least an order of magnitude larger than the dye molecule studied in our system. The lateral diffusion constant of fluorescence-labeled lipids on supported phospholipid membranes was found to be 3.5×10^{-8} cm^2/s.[46] Tracer (dye molecule) diffusion in a free-standing smectic liquid crystal was found to have a diffusion constant of 8×10^{-8} cm^2/s in films 4 molecules thick.[14] These systems are similar to ours in that they are all two-dimensional small molecule systems. The diffusion rates reported for the lipid bilayer and liquid-crystal film are similar to the diffusion constants we found for prodan diffusion on CTS and PEG surfaces. As mentioned above, the lipid experiments are fundamentally different from ours in that the diffusing molecules and the medium are the same, and both are mobile. The diffusing and medium molecules in the tracer−liquid-crystal system are chemically different, but again, the medium molecules are able to diffuse. Apparently, the immobility of the medium in our system does not significantly limit the mobility of the diffusing species. This is another indication that the important parameters for our system are the interaction of the diffusing species with the medium, the free volume of the medium, and, perhaps for the grafted-polymer case, the mobility of the polymer segments.

Conclusions

FRAP is used to determine diffusion constants for the dye prodan on clean glass, SAMs formed from CTS and OTS, and PEG grafted to silica. Similar diffusion constants are found for the CTS and PEG layers, which is thought to be due at least in part to the ability of prodan to partially intercalate in these layers enabling good dispersion and diffusion. No fluorescence recovery is observed on the OTS SAM or on the clean silica surface. Dye is thought to aggregate on the former and form hydrogen bonds with and possibly aggregate on the latter. Importantly, in systems where diffusion is observed, prodan diffusion is determined to take place on the various surfaces and not through the gas phase. There is no significant change in the rate of diffusion with relative humidity on the PEG layer, but there is a slight increase on the CTS SAM. The fluorescence intensity as well as the degree of unrecoverable fluorescence of prodan after photobleaching on the PEG surface increases with relative humidity at high dye concentrations, indicating some degree of aggregation on PEG surfaces at higher dye concentrations. Future studies will also include printing patterned layers on a surface, which will be important for the realization of many applications.

Acknowledgment. This work was supported in part by a Young Investigator award from the Arnold and Mabel Beckman Foundation, the NIRT Initiative of the NSF under Award No. CHE-0103447, and the U.S. Department of Energy, Division of Materials Sciences under Award No. DEFG02-91ER45439, through the Frederick Seitz Materials Research Laboratory at the University of Illinois at Urbana−Champaign. Ellipsometry data were obtained in the Laser and Spectroscopy Facility at the Frederick Seitz Materials Research Laboratory. We gratefully acknowledge the support of the Beckman Institute ITG, especially K. Garsha and Dr. G. Fried with confocal microscopy and D. Webber with programming and general computer assistance. We thank S. Park for his help with derivation of diffusion equations and Mathematica and Y.-J. Lee for assistance with UV−vis absorption spectroscopy.

Supporting Information Available: The C computer program used to analyze FRAP images and derivation of eq 5. This material is available free of charge via the Internet at http://pubs.acs.org.

References and Notes

(1) Morgenstern, K.; Laegsgaard, E.; Besenbacher, F. *Phys. Rev. Lett.* **2001**, *86*, 5739.
(2) Oh, S.-M.; Koh, S. J.; Kyuno, K.; Ehrlich, G. *Phys. Rev. Lett.* **2002**, *88*, 236102.
(3) Boxer, S. G. *Curr. Opin. Chem. Biol.* **2000**, *4*, 704.
(4) Maier, B.; Radler, J. O. *Phys. Rev. Lett.* **1999**, *82*, 1911.
(5) Perera, D. N.; Harrowell, P. *Phys. Rev. Lett.* **1998**, *80*, 4446.
(6) Luo, L.-S.; Phillies, G. D. *J. Chem. Phys.* **1996**, *105*, 598.
(7) Pertsinidis, A.; Ling, X. *Nature* **2001**, *413*, 147.
(8) Schwartz, D. *Annu. Rev. Phys. Chem.* **2001**, *52*, 107.
(9) Bishop, A.; Nuzzo, R. *Curr. Opin. Colloid Interface Sci.* **1996**, *1*, 127.
(10) Axelrod, D. *Biophotonics, Part B* **2003**, *361*, 1.
(11) Cubeddu, R.; Comelli, D.; D'Andrea, C.; Taroni, P.; Valentini, G. *J. Phys. D: Appl. Phys.* **2002**, *35*, R61.
(12) Taki, S.; Ishida, K.; Okabe, H.; Matsushige, K. *J. Cryst. Growth* **1993**, *131*, 13.
(13) Yang, G.; Gy, L. *J. Phys. Chem. B* **2003**, *107*, 8746.
(14) Bechhoefer, J.; Geminard, J.-C.; Bocquet, L.; Oswald, P. *Phys. Rev. Lett.* **1997**, *79*, 4922.
(15) Blume, A. *Curr. Opin. Colloid Interface Sci.* **1996**, *1*, 64.
(16) Sukhishvili, S.; Chen, Y.; Muller, J.; Gratton, E.; Schweizer, K.; Granick, S. *Macromolecules* **2002**, *35*, 1776.
(17) Sukhishvili, S.; Chen, Y.; Muller, J.; Gratton, E.; Schweizer, K.; Granick, S. *Nature* **2000**, *406*, 146.
(18) Perkins, I.; Smith, D.; Chu, S. *Science* **1994**, *264*, 819.
(19) Hall, D.; Torkelson, J. *Macromolecules* **1998**, *31*, 8817.
(20) Hall, D.; Deppe, D.; Hamilton, K.; Dhinojwala, A.; Torkelson, J. *J. Non-Cryst. Solids* **1998**, *235*, 48.
(21) Muller, J.; Chen, Y.; Gratton, E. *Biophotonics, Part B* **2003**, *361*, 69.
(22) Schwille, P.; Korlach, J.; Webb, W. *Cytometry* **1999**, *36*, 176.
(23) Ikeda, Y. *J. Appl. Polym. Sci.* **2000**, *78*, 1530.
(24) Ferry, J. *Viscoelastic Properties of Polymers*; Wiley: New York, 1980.
(25) Laschitsch, A.; Bouchard, C.; Habicht, J.; Schimmel, M.; Ruhe, J.; Johannsmann, D. *Macromolecules* **1999**, *32*, 1244.
(26) Biesalski, M.; Ruhe, J. *Langmuir* **2000**, *16*, 1943.
(27) Cras, J.; Rowe-Taitt, C.; Nivens, D.; Ligler, F. *Biosens. Bioelectron.* **1999**, *14*, 683.
(28) Xia, Y.; Whitesides, G. *Annu. Rev. Mater. Sci.* **1998**, *28*, 153.
(29) Jeon, N.; Choi, I.; Whitesides, G.; Kim, N.; Laibinis, P.; Harada, Y.; Finnie, K.; Girolami, G.; Nuzzo, R. *Appl. Phys. Lett.* **1999**, *75*, 4201.
(30) Leggett, G.; Sun, S. *Nano Lett.* **2002**, *2*, 1223.
(31) Becker, H.; Gartner, C. *Electrophoresis* **2000**, *21*, 12.
(32) Guo, T.; Chang, S.; Pyo, S.; Yang, Y. *Langmuir* **2002**, *18*, 8142.
(33) Jo, S.; Park, K. *Biomaterials* **2000**, *21*, 605.
(34) Zalipsky, S.; Gilon, C.; Zilkha, A. *Eur. Polym. J.* **1983**, *19*, 1177.
(35) Lakowicz, J. *Principles of Fluorescence Spectroscopy*, 2nd ed.; Kluwer Academic/Plenum Publishers: New York, 1999.
(36) Haugland, R. *Handbook of Molecular Probes and Research Products*; Molecular Probes: Eugene, 2003.
(37) Brinker, C.; Scherer, G. *Sol-Gel Science: The Physics and Chemistry of Sol-Gel Processing*; Academic Press: San Diego, 1990.
(38) Lide, D. *CRC Handbook of Chemistry and Physics*, 81st ed.; CRC Press: Boca Raton, 2000−2001.
(39) Haas, D.; Quijada, J.; Picone, S.; Birnie, D. I. *SPIE Proc.* **2000**, *3943*, 280.
(40) Weber, G.; Farris, F. J. *Biochemistry* **1979**, *18*, 3075.
(41) Crank, J. *The Mathematics of Diffusion*; Oxford University Press: London, 1975.
(42) Entwistle, A.; Noble, M. *J. Microsc.* **1992**, *165*, 331.
(43) Forster, T.; Konig, E. *Z. Electrochem.* **1957**, *61*, 344.
(44) Stevens, M. J. *Langmuir* **1999**, *15*, 2773.
(45) Ulman, A. *An Introduction to Ultrathin Organic Films from Langmuir-Blodgett to Self-Assembly*; Academic Press: San Diego, 1991.
(46) Harms, G.; Sonnleitner, M.; Schutz, G.; Gruber, H.; Schmidt, T. *Biophys. J.* **1999**, *77*, 2864.